Synthesis, Properties and Biomedical Applications of Novel Core-Shell Iron Magnetic Nanoparticles

You Qiang*, Amit Sharma, Daniel Meyer, Jiji Antony, Muhammad Faheem, Jamie Hass, Alan McConnaughey, Ryan Souza and Michael Campanell

Department of Physics, University of Idaho, Moscow, ID 83844-0903,

*Corresponding author: *E-mail: youqiang@uidaho.edu, Telephone: (208) 885-7558, Fax: (208) 885-4055*

ABSTRACT

Nanoparticles have gained increased attention recently for biomedical applications. Biocompatible magnetic nanoparticles (MNPs) have been found promising in several biomedical applications for tagging, imaging, drug delivery, sensing and separation in recent years. Most magnetic particles or beads currently used in biomedical applications are based on iron oxides with very low specific magnetic moments of ~30 emu/g. In this presentation, we report room-temperature synthesis of novel iron-iron oxide core-shell nanoclusters using a newly developed nanocluster source. Monodispersive iron nanoclusters with size of diameters from 1 to 100 nm are produced in a source chamber and then transmitted into the reaction chamber where a small partial pressure of O_2 is present so that the nanoclusters are coated with uniform iron oxide shell. These shells act as passivation layers preventing further oxidation of the cores upon subsequent or continued exposure to air. The size of core-shell nanoclusters varies with the He:Ar ratio, chamber pressure, and growth distance through the aggregation tube. The clusters were characterized by XPS, XRD and HRTEM. The bcc-Fe core with magnetite shells was observed by XRD and HRTEM. The core-shell nanoclusters are superparamagnetic at room temperature for sizes less than 15 nm, and then become ferromagnetic when the cluster size increases. The specific magnetic moment of core-shell MNPs is size dependent, and increases rapidly from about 80 emu/g at the cluster size of around 3 nm to over 200 emu/g up to the size of 100 nm. The use of high magnetic moment nanoclusters for biomedical applications could dramatically enhance the contrast for MRI, reduce the concentration of magnetic particle needs for cell separation, or make drug delivery possible with much lower magnetic field gradients. These MNPs were incubated and successfully untaken by lung cancer cells for the toxicity.

Keywords: core-shell nanoparticle, synthesis, magnetism, biomedical application

1 INTRUDUCTION

Nanoclusters are ultrafine particles of nanometer dimensions located in the transition region between molecules and microscopic structures. Viewed as molecules, they are so large that they provide access to realms of quantum behavior that are not otherwise accessible; viewed as bulk materials, they are so small that they exhibit characteristics that are not observed in larger (even 100 nm) structures. It is in this size regime that many recent advances have been made in biology, physics, and chemistry [1-5]. Since their introduction in the mid-1970s, magnetic particles (micro-beads and ferrofluids) have been widely studied for their applications in various fields in biology and medicine such as magnetic targeting (drugs, genes, radio-pharmaceuticals), magnetic resonance imaging (MRI), diagnostics, immunoassays, RNA and DNA purification, cell separation and purification as well as hyperthermia generation [1, 6-7]. Nanotechnology is beginning to allow scientists, engineers, and physicians to work at the cellular and molecular levels to produce major advances in the life sciences and healthcare.

Iron oxide particles such as magnetite *(Fe_3O_4)* or maghemite *(γ-Fe_2O_3)* are by far the most commonly employed for biomedical applications. Highly magnetic materials such as cobalt and nickel are toxic, susceptible to oxidation and hence are of little interest. Moreover, the main advantage of using particles of sizes smaller than 100 nm is their higher effective surface areas (easier attachment of ligands), lower sedimentation rates (high stability) and improved tissular diffusion [10-12]. Therefore, for *in vivo* biomedical applications, MNPs must be made of a non-toxic and non-immunogenic material, with particle sizes small enough to remain in the circulation after injection and to pass through the capillary systems of organs and tissues avoiding vessel embolism. They must also have a high magnetization so that their movement in the blood can be controlled with a relative small magnetic field and so that they can be immobilized close to the targeted pathologic tissue [8-9].

For *in vitro* applications the size restrictions are not so severe as in *in vivo* applications. Therefore, composites consisting of superparamagnetic nanocrystals dispersed in submicron diamagnetic particles with long sedimentation times in the absence of a magnetic field can be used. The advantage of using diamagnetic matrixes is that the superparamagnetic composites can be easily provided with functionality.

For biomedical applications the use of particles that present superparamagnetic behavior at room temperature (no remanence along with a rapidly changing magnetic state) is preferred. Furthermore, applications in biology and medical diagnosis and therapy require the MNPs to be stable in water at neutral pH and physiological salinity.

In almost all applications the preparation method of the nanomaterials represents one of the most important

challenges that will determine the particle size and shape, the size distribution, the surface chemistry of the particles and consequently their magnetic properties. Recently many attempts have been made to develop processes and techniques that would yield 'monodispersed colloids' consisting of uniform nanoparticles both in size and shape [11, 19-20]. Monodispersed colloids have been exploited in fundamental research and as models in the quantitative assessment of properties that depend on the particle size and shape. In addition, it has become evident that the quality and reproducibility of commercial products can be more readily achieved by starting with well-defined MNPs of known properties.

Oxide MNPs coated with compounds such as dextran or starch for biocompatibility are now widely used [1-10, 18-21]. Ferrite nanoparticles are biocompatible and easily synthesized, but the specific magnetic moment of ferromagnetic iron oxide particles is very low. Most MNPs used currently are based on ferromagnetic iron oxides with low specific magnetic moment of about 20–30 emu/g. Iron has a greater specific magnetization than either of these iron oxides. The problem is that pure metallic iron nanoparticles are highly sensitive to oxidation and dissolution through electrochemical reactions. If iron nanoparticles were passivated with a thin ion oxide shell and retain the high magnetic moments of pure iron cores, they will dramatically enhance the contrast for MRI, reduce the concentration of magnetic particles needed for cell separation, or make drug delivery possible with much lower magnetic field gradients.

To realize this goal, we apply a new approach of our newly developed nanocluster deposition system to synthesize monodispersive, high specific magnetic moment core-shell nanostructured clusters.

2 EXPERIMENT

The MNPs are deposited by newly developed nanocluster deposition system using a combination of magnetron-sputtering and gas–aggregation techniques [13-17]. The cluster beam deposition apparatus is mainly composed of three parts: a cluster source, an e-beam evaporation chamber and a deposition chamber. The sputtered Fe atoms from a high-pressure magnetron-sputtering gun are decelerated by collisions with Ar gas (the flow rate: 100–500 sccm) injected continuously into the cluster growth chamber, which is cooled by chilled water. The clusters formed in this chamber are ejected from a small nozzle by differential pumping and a part of the cluster beam is intercepted by a skimmer, and then deposited onto a sample holder in the deposition chamber. The mean size of clusters, from 1 nm to 100 nm, is easily varied by adjusting the aggregation distance, the sputter power, the pressure in the aggregation tube, and the ratio of He to Ar gas flow rate. The aggregation distance and the ratio of He to Ar gas flow rate are important parameters for getting a very high intensity (> 5 Å/s), monodispersed nanocluster beam. A major advantage of this type of system is that the clusters have much smaller size dispersion than grains obtained in any typical vapor deposition system. Studies with TEM and time-of-flight (TOF) mass spectrometer have shown that the observed lognormal size distribution has a standard deviation less than 8%. When oxygen gas is introduced into the deposition chamber during processing, uniform iron oxide shells covering the Fe clusters are formed.

Fe nanoclusters of variable mean size of diameters from 1 to 100 nm are generated by the nanocluster source, which combines an improved high-pressure magnetron-sputtering gun with a gas-aggregation tube cooled by chilled water. We can control the cluster size by changing the flow rate of Ar gas (R_{Ar}), the flow rate of He gas (R_{He}), and the cluster growth length (L). One of the conditions to form a thick film of iron-iron oxide core-shell nanoclusters is to apply a power of 200 watts to the sputtering gun, when flow rate in the aggregation tube is 126 sccm of He and 564 sccm of Ar for about an hour. We are able to prepare up to 20 mg per hour of monodispersive nanoclusters for each size. For the preparation of Fe oxide-coated Fe clusters, we introduced oxygen gas at a flow rate around 4 sccm into the deposition chamber through a nozzle set behind the skimmer. Inside the deposition chamber, a chemical reaction began that formed iron oxide shells which covered the Fe clusters before they were deposited on the substrate. The clusters landed softly on the surface of substrates at room temperature and retain their original shape. This process ensures that all Fe clusters are uniformly oxidized before the cluster films are formed. We make a starch thin film on the surface of Si wafer, and then deposit the Fe clusters on the top of the starch film. The iron clusters can be easily dissolved and suspended in warm water for further bio-molecule conjugations.

Three kinds of substrates are used for the core-shell cluster analysis: microgrids for TEM observations, silicon wafers for AFM, and polyimide films for magnetic measurement. Magnetic measurement was performed using a superconducting quantum interference device magnetometer (SQUID of MPMS XL-7) between 2 and 400 K with the maximum field of 70 kOe.

3 RESULTS AND DISCUSSION

Figure 1A shows a TEM image of the core-shell nanoclusters. The mean cluster diameter is 6.65 nm. The standard deviation is less than 7%. The distribution fits well to a lognormal function with a very narrow size distribution. Our results clearly demonstrate that monodispersive nanoclusters in the size range of around 1–100 nm are reproducible by choosing the appropriate growth parameters R_{Ar}, R_{he}, and L.

Figure 1B shows high-resolution TEM (HRTEM) overviews of 4 single core-shell structured nanoclusters with size range from 3 nm to 85 nm deposited on a carbon film of microgrids. The nanoparticles appear almost spherical, and those that have a crystal axis oriented along the electron beam direction show two contrasts, a dark iron core region and a light-gray oxide shell. The electron

diffraction pattern obtained from a large sample area tells us the core has the bulk iron bcc lattice structure with the lattice fringe 0.286 nm. The HRTEM results also indicate that the oxide-coated Fe nanoclusters were covered uniformly with the shells composed of very small nanocrystallites.

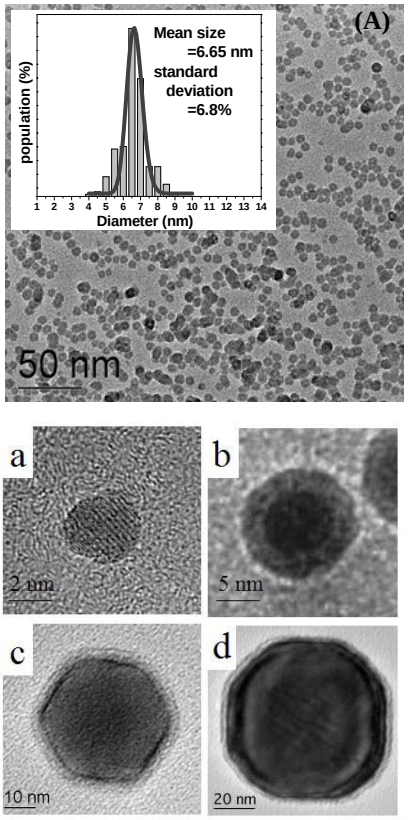

Fig. 1: (A) A low resolution TEM image of the iron-iron oxide core-shell nanoclusters and the insert gives a plot for size distribution; (B) HRTEM micrographs of the oxide-coated Fe clusters with diameter from around 3 nm to 85 nm prepared on carbon microgrids

The iron oxide shell has a thickness of about 2.5 nm independent of the nanoparticle size. We observed that the core-shell nanoclusters are very stable against further oxidation after a long time exposure to air. According to our HRTEM measurements the shell thickness remains no change after the nanoclusters exposure to air more than 6 months. When we annealed the samples at 250 C degree for 3 hours in the air, the shell thickness has increased to about 5 nm with slightly decreasing of the core size but the core-shell nanostructures remain intact. For sizes smaller than 7 nm, there are no core-shell structures (Fig. 1B-a) because the oxidation goes through the entire nanoparticle.

Figure 2 shows hysteresis loops of Fe oxide-coated nanoclusters at room temperature. The samples with cluster size less than 15 nm are superparamagnetic at room temperature without coercivity. Fig. 2-a is one example of a cluster size of 10 nm. The field-cooling and zero-field-cooling measurements tell us the block temperature is about 45 K. It is clear that this cluster exhibits superparamagnetic behavior. When the sizes of clusters are larger than 15 nm, they are ferromagnetic. The coercivity increases from 25 Oe for 15 nm size clusters to about 1 kOe for 100 nm clusters. Fig. 2-b shows a typical hysteresis loop of 85 nm diameter clusters with H_c = 890 Oe. Even at 4 T, the hysteresis loop has not been saturated due to many very small iron oxide nano-crystallites in the uniform shells. Those nano-crystallites are superparamagnetic at room temperature. All the samples at low temperature (4 K) are magnetically ordered with hysteresis loops and H_c is from 0.4 to 1.5 kOe as cluster sizes increase. We obtain the saturated magnetization (M_s) by a high-field fit to the expression $M = M_s (1-A/H^2)$, where A is a constant and H is the applied field. The results of M_s divided by the weight of the cluster films provide the specific magnetic moments with a unit of emu/g.

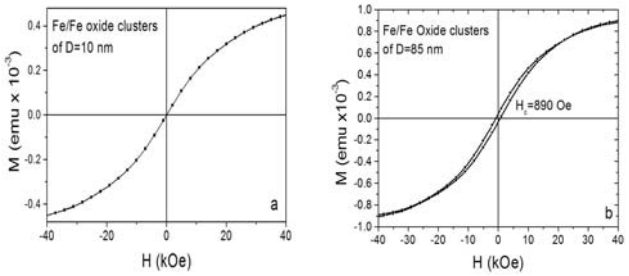

Fig. 2: Hysteresis loops of Fe oxide-coated Fe clusters with (a) D = 10 nm and (b) D = 85 nm at room temperature.

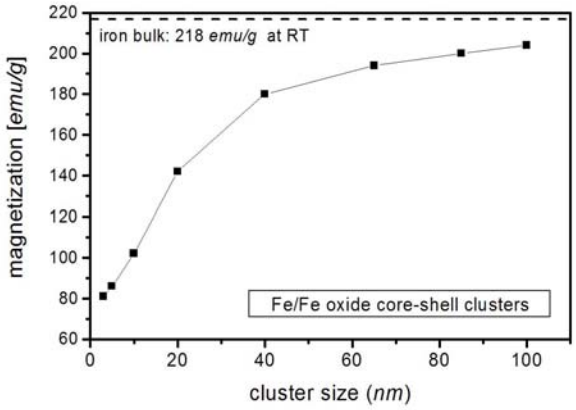

Fig. 3: Size dependent specific magnetic moments of Fe oxide-coated Fe nanoclusters.

Figure 3 shows a curve of the specific magnetic moment versus the nanocluster size. It can be seen that it increases as cluster size increases from 3 nm to 100 nm. When the size is less than 10 nm, the specific magnetic moment is around 80 emu/g, similar to the value of ferromagnetic iron oxides-magnetite. This information is consistent with the HRTEM image, which shows that the entire nanocluster is oxidized to form a superparamagnetic iron oxide

nanoparticle. If the cluster size is larger than 10 nm, the value of the specific magnetic moment increases dramatically until the cluster size reaches 100 nm where it almost saturates at 205 emu/g. This is close to the pure bulk Fe value (218 emu/g). This value is almost 10 times larger than the value (20-30 emu/g) for iron oxide nanoparticles currently used in biomedical applications.

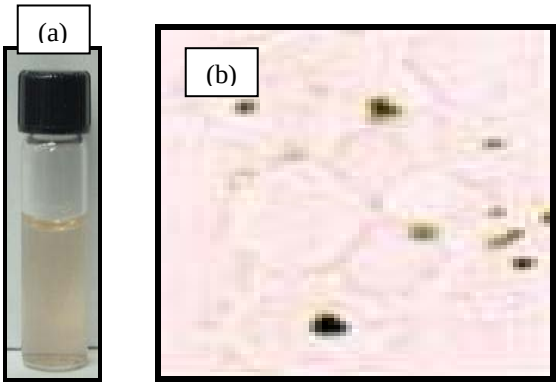

Fig. 4: (a) is the image of the nanoparticles uniformly dissolved in the solution of pH 7; (b) Dextrin coated MNPs incubated with lung cancer cells.

The MNPs were removed from the substrate surface and collected in the solution of pH 7. Fig. 4(a) is an image of nanoparticles uniformly dissolved in the solution. Fig. 4(b) shows dextrin coated MNPs incubated with lung cancer cells. Results indicate that MNPs coated with dextrin are untaken by the cancer cells, indicating that MNPs are not toxic.

4 SUMMARY

In summary, monodispersive core-shell nanostructured clusters with high specific magnetic moments (about 200 emu/g) are synthesized by a new approach of the nanocluster deposition system. The size of core-shell nanoclusters can be changed easily from 2 nm to 100 nm by controlling the growth parameters. HRTEM images show the coatings are iron oxides which very uniformly cover the Fe cores. The nanoclusters of size less than 15 nm are superparamagnetic at room temperature and become ferromagnetic with increasing size. The specific magnetic moment of core-shell nanoclusters is size dependent, and increases rapidly from about 80 emu/g at the cluster size of around 3 nm to over 200 emu/g at the size of 100 nm. The use of high magnetic moment nanoclusters for biomedical applications could dramatically enhance the contrast for MRI, reduce the concentration of magnetic particle needs for cell separation, or make drug delivery possible with much lower magnetic field gradients.

5 ACKNOWLEDGMENTS

Financial support from NIH-INBRE and DOE-BES (DE-FG02-06ER15777) is gratefully acknowledged. TEM data was collected at EMSL, a user facility sponsored by the DOE and operated by Battelle. Dr. Chongmin Wang at PNNL is thanked for highly valuable TEM assistance.

REFERENCES

1. *Andra, W. and Nowak, H. "Magnetism in Medicine", Wiley-VCH, Berlin, 1998*
2. *Brigger, I.; Dubernet, C.; Couvreur, P. Adv. Drug Delivery Rev.* ***2002****, 54631-51.*
3. *Whitesides G and Alivisatos A P 1999 Fundamental scientific issues for nanotechnology Nanotechnology Research Directions ed A P Alivisatos et al (IWGN Workshop Report)*
4. *Cancer Nanotechnology Plan, National Institutes of Health, National Cancer Institute, July 2004.*
5. *Fritzsche, W. and T. A. Taton. 2003. Nanotechnol. 14:R63-R73.*
6. *Hadjipanayis, G.C. Siegel, R.W. (Eds.), Nanophase Materials, Kluwer, Dordrecht, 1994.*
7. *Haefeli, U. Schuett, W. Teller, J. Zborowski M. (Eds.), Scientific and Clinical Applications of Magnetic Carriers, Plenum Press, New York, 1997.*
8. *Hatch G. P. and R. E. Stelter, J. Magn. Magn. Mater., 225 (2001) 262-276.*
9. *Jordan A, Scholz R, et. al. 2001 J. Magn. Magn. Mater.* ***225****, 118*
10. *Kim Do K., M. Mikhaylova, Y. Zhang and M. Muhammed, Chem. Mater, 15 (2003) 1617-1627.*
11. *Matijevic E (ed) 1989 Fine Particles A special issue in MRS Bulletin* ***14*** *18; 1993 Chem. Mater.* ***5*** *412*
12. *Portet D, Denizot B, Rump E, Lejeune J J and Jallet P 2001. J. Colloid Interface Sci.* ***238*** *37*
13. *Qiang, You, Jiji Antony, Amit Sharma, Sweta Pendyala, Joe Nutting, Daniel Sikes and Daniel Meyer, J. of Nanoparticle Research, 8 (2006) 489.*
14. *Antony, Jiji, You Qiang, Donald R. Baer and Chongmin Wang, J. of Nanoscience and Nanotechnology, 6, 568-572 (2006).*
15. *Qiang, Y. R. F. Sabiryanov, S. S. Jaswal, Y. Liu, H. Haberland, and D. J. Sellmyer, Phys. Rev. B 66, 064404 (2002).*
16. *Qiang, Y. J. Antony, M. G. Marino, and S. Pendyala. IEEE Trans. Magnet. 40(2004)6, 3538-3540.*
17. *Antony, J., X.B. Chen, J. Morrison, L. Bergman, Y. Qiang, D.E. McCready, and M. Engelhard, Appl. Phys. Letters, 87, 241917, 2005.*
18. *Reich, D. H. et. al., J. Appl. Phys., vol.93, 7275-7280 (2003)*
19. *Sugimoto T 2000 Fine Particles: Synthesis, Characterization and Mechanism of Growth (New York: Marcel Dekker)*
20. *Tada, M. S. Hatanaka, H. Sanbonsugi, N. Matsushita and M. Abe, J. Appl. Phys., vol.93, 7566-7568 (2003).*
21. *Zhao, M., M. F. Kircher, L. Josephson, and R. Weissleder. 2002. Bioconjug. Chem. 13:840-844.*